Deep-Sea Research Part I xxx (xxxx) xxx–xxx

Contents lists available at ScienceDirect

Deep-Sea Research Part I

journal homepage: www.elsevier.com/locate/dsri

Seismic airgun sound propagation in Arctic Ocean waveguides

Kelly A. Keen, Bruce J. Thayre, John A. Hildebrand, Sean M. Wiggins*

Scripps Institution of Oceanography, 9500 Gilman Drive, La Jolla, CA 92093-0205, United States

ARTICLE INFO

Keywords:
Arctic Ocean
Noise pollution
Seismic airguns
Sound propagation

ABSTRACT

Underwater recordings of seismic airgun surveys in the deep-water Beaufort Sea and on the shallow-water Chukchi Sea shelf were made from sites on the continental slope and shelf break north-northwest of Point Barrow, Alaska. Airgun pulses from the deep-water survey were recorded more than 500 km away, and from the shallow-water survey up to ~100 km. In the deep-water, received sound pressure levels show spherical spreading propagation; whereas, sound exposure levels exhibit cylindrical spreading propagation. Over the shallow-water shelf, transmission losses were much greater than spherical spreading, due to energy loss in the seafloor. Understanding how sound propagates across large spatial scales in the Arctic Ocean is important for better management and mitigation of anthropogenic noise pollution in marine soundscapes, especially as diminished ice in the Arctic Ocean allows for longer range sound propagation.

1. Introduction

Declining sea ice provides increased access to the Arctic, raising concerns about future levels of anthropogenic noise pollution and how it may affect wildlife. Of increasing interest are seismic surveys occurring in the Beaufort and Chukchi Seas (Fig. 1), which utilize airgun arrays to acquire information about sub-seafloor features, including oil and gas reserves and other geologic structures. Airgun arrays generate repeatable pulses with source sound pressure levels up to 260 dB_{pp} re 1 μPa @ 1 m (peak-to-peak) in the frequency band from 5 to 300 Hz (Turner et al., 2006). Although these pulses are directed at the seafloor, acoustic energy also radiates horizontally (Dragoset, 1984, 2000), ensonifying the water column and creating increased noise levels (e.g., Roth et al., 2012). Because of the high source levels and low-frequency content of airgun arrays (Hildebrand, 2009), seismic pulses have been detected at hundreds or even thousands of kilometers range (Thode et al., 2010; Nieukirk et al., 2004). Environmental factors that produce acoustic waveguides, with low sound transmission losses, facilitate the spread of noise pollution over a wide area.

In the deep waters of the Arctic Ocean and other polar regions where cold surface water temperatures are nearly constant with depth, sound velocity generally increases with depth from the surface to the bottom. Under these conditions, a sound channel is created by upward refraction in the water column and by repeated reflection from the sea surface. When ice is present, scattering from its rough canopy limits the long-range propagation of sound to only low frequencies (< ~40 Hz). Much of the work on Arctic propagation to date has been focused on ice-covered waters and the excess scattering that occurs as the signal interacts with the rough underside of the ice (Marsh and Mellen, 1963; Buck and Greene, 1964; DiNapoli and Mellen, 1986; LePage and Schmidt, 1994; Gavrilov and Mikhalevsky, 2006). With climate change leading to diminishing ice cover, studies have begun to examine propagation under ice-free conditions (Thode et al., 2010), and have found substantially higher amplitude long-range sound propagation.

In the deep-water Beaufort Sea, the near-surface acoustic waveguide minimizes the effects of bottom topography on sound propagation and contributes to long-range refractive propagation with reduced transmission loss (Yang, 1984; Thode et al., 2010). In comparison, the shallow-water Chukchi Sea creates an acoustic waveguide between the seafloor and sea surface. In this case, sound propagation is dominated by the signal's reflections with the seafloor and sea surface, but its interaction with the sub-seafloor sediments can also influence the propagation distance (Ireland et al., 2007; Gavrilov and Mikhalevsky, 2006; Bongiovanni et al., 1995).

As a seismic pulse propagates in an acoustic waveguide, it becomes increasingly distorted due to dispersion. In both shallow-water and near-surface waveguides, each normal mode has a distinctive dispersion curve, describing how different frequencies travel at different velocities, allowing the dispersion to be modeled (e.g. Medwin and Clay, 1998; Jensen et al., 2000). With known source signals, their dispersion can be used to estimate the distance between the source and the receiver (e.g., Wiggins et al., 2004; Munger et al., 2011).

In this study, we use normal mode dispersion modeling (NMDM) to estimate ranges to seismic airgun surveys in the deep-water Beaufort

* Corresponding author.
E-mail address: swiggins@ucsd.edu (S.M. Wiggins).

https://doi.org/10.1016/j.dsr.2018.09.003
Received 6 March 2018; Received in revised form 7 September 2018; Accepted 7 September 2018
0967-0637/

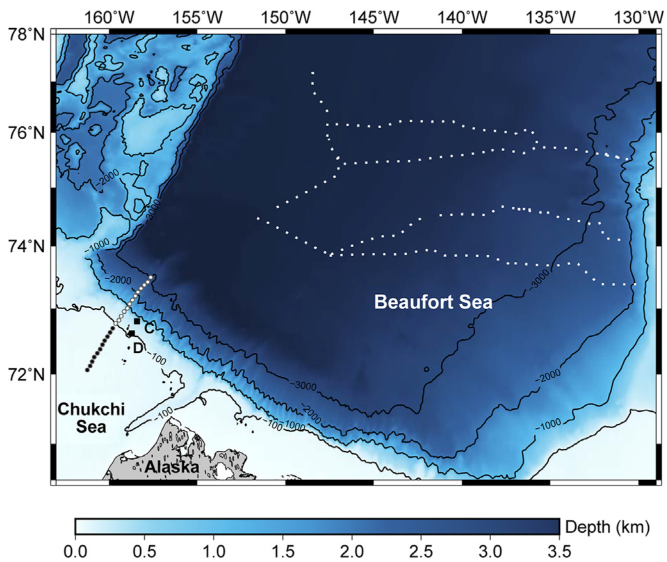

Fig. 1. Bathymetric map of the study site including the Beaufort Sea and Chukchi Sea. The white dots in the deep-water Beaufort Basin represent track lines completed by the Canadian Coast Guard Ship *Louis S. St-Laurent* (*LSSL*) during a geophysical seismic survey conducted in 2007. The circles on the shallow-water Chukchi Shelf represent the track line completed by M/V *Norseman*, the marine mammal passive acoustic monitoring vessel that accompanied the airgun survey vessel R/V *Geo Arctic* during the 2013 survey. The black circles represent the portion of the survey line used for analysis, and the white circles represent the omitted portion of the line that did not exhibit shallow-water waveguide normal mode dispersion. The black squares (C and D) represent the high-frequency acoustic recording package (HARP) deployment sites near the shelf break. Black bathymetric contours are at 100, 1000, 2000, and 3000 m depths with darker shading indicating deeper depths.

Sea and on the Chukchi Sea shelf from single long-term autonomous acoustic recorders deployed on the continental shelf and slope break north-northwest of Point Barrow, Alaska. Source-receiver range estimates were also obtained from seismic survey reports allowing NMDM range estimates to be validated. Knowledge of the source-receiver range allowed for the examination of waveguide sound transmission loss in deep-water and on the shelf using both sound pressure levels and sound exposure levels measured from these recordings. Sound transmission loss estimates are important for defining affected areas in managing noise pollution for marine soundscapes.

2. Methods

2.1. Acoustic measurements and analysis

To record natural and man-made underwater sounds over long periods, two high-frequency acoustic recording packages (HARPs; Wiggins and Hildebrand, 2007) were deployed in the Arctic (Fig. 1). One HARP was deployed in 2007 north-northwest of Point Barrow, Alaska on the continental slope between the Chukchi Shelf and Beaufort Basin at a depth of 328 m (Site C). Another HARP was deployed in 2013 on the shelf southwest of Site C at a depth of 100 m (Site D). HARPs consist of a tethered hydrophone sensor buoyed above the seafloor ~10 m or more, low-power data acquisition system with large data storage (~2 and ~5 TB for 2007 and 2013, respectively), batteries, electronic housings, flotation, and acoustic release system to jettison ballast which is used to fix the instrument to the seafloor until instrument recovery.

In 2007, the HARP recorded with a schedule of approximately 7 min out of every 14 min using a 32-kHz sample rate and 16-bit digitizer. In 2013, the HARP recorded with a schedule of approximately 10 min out of every 15 min using the same digitizer sampling at 200 kHz. During open-water conditions in the late summer or early fall, the HARPs were recovered to retrieve the recordings, renovated with new data storage hard disk drives, batteries and ballast, and redeployed to the seafloor. HARP hydrophone calibrations were conducted at Scripps Institution of Oceanography and at the U.S. Navy's Transducer Evaluation Center (TRANSDEC) in San Diego, California. TRANSDEC calibrations confirmed the predicted hydrophone response, based on laboratory measurements of the preamplifier electronics with 40 dB of gain and the manufacturer-specified sensitivity of the hydrophone transducers (−202 dB re V/μPa), to be within ± 1–2 dB of the calibration measured response.

Raw data from these instruments were processed into XWAV format files that are similar to standard lossless audio WAV format, but include additional information in an expanded header (Wiggins and Hildebrand, 2007). Acoustic analysis of XWAVs was accomplished using a MATLAB-based (The MathWorks Inc., Natick, MA) program *Triton* (Wiggins and Hildebrand, 2007) to view spectrograms of XWAV files, playback recorded sounds, and log start and end times of seismic airgun pulses. Sound pressure spectrum level and spectrogram plots for the HARP data were calculated using the Welch method (Welch, 1967), with Hann windows, 1 Hz frequency bins, and 0% overlap for spectrum and 95% overlap for spectrogram plots.

During seismic airgun surveys, wave trains of sequential airgun pulses typically occur for long periods (hours to days) with a constant inter-pulse interval of 10's of seconds. When the seismic source is far away from the recorder (100's of km), received signals are similar for many hours because survey ship speeds (~8 km h^{-1}) do not result in a significant change in range (Roth et al., 2012).

For the deep-water survey in 2007, start and end times of 20 successive seismic pulses were logged every 224 min to investigate potential changes in the received signal of the seismic source. This time period for pulse evaluation was chosen to accommodate 16 complete 7-min windows based on the instrument's 50% recording schedule. Masking, attenuation and other factors often made it difficult to log all 20 successive pulses in an evaluation time period. If a bout of 20 pulses could not be logged every 224 min, another bout was selected before or after to fill in gaps between logged bouts.

For the shallow-water survey in 2013, the seismic survey line analyzed was shorter in time and distance covered, so start and end times were logged more frequently with 10 airgun signals every 15 min for the duration of the survey line. Only signals exhibiting clear modal separation were selected for analysis, reducing the pulses evaluated to those originating from on the shelf at water depths less than 100 m (Fig. 1; black circles).

Airgun signals are impulsive, so it is often preferable to measure their amplitude as peak-to-peak (PP) or zero-to-peak (i.e., peak [P]) sound pressure level (SPL) rather than root-mean-square (RMS), which typically is used to measure continuous or nearly continuous signals. The RMS SPL of a long duration sinusoid signal is 9 dB below its PP SPL, but for a pulsed signal, the RMS SPL can be 20 dB or more below the PP SPL and is sensitive to signal duration (Madsen, 2005). RMS SPL was calculated from the square of the instantaneous pressure, P(t), of the signal at time t integrated and averaged over the signal duration (T) and reference pressure $P_{ref} = 1$ μPa:

$$\mathrm{RMS} = 10 \times \log_{10}\left(\frac{1}{T}\frac{\int_0^T P(t)^2 dt}{P_{ref}^2}\right) = 10 \times \log_{10}\left(\frac{\int_0^T P(t)^2 dt}{P_{ref}^2}\right) - 10 \times \log_{10}(T) \quad (1)$$

In a regime of dispersive propagation, the total duration of the seismic signal increases with propagation range as the initial impulse is broadened to become more sinusoidal and extended in time. Under these circumstances, sound exposure level (SEL) is a useful metric to capture the total extent of the pulse, essentially retaining the energy that is contained within the longer pulse duration. SEL accounts for the total energy within a sound by using the cumulative sum of the squared pressure over the duration of the sound (e.g., Southall et al., 2007; Munger et al., 2011):

$$\mathrm{SEL} = 10 \times \log_{10}\left(\frac{\int_0^T P(t)^2 dt}{P_{ref}^2}\right) = \mathrm{RMS} + 10 \times \log_{10}(T) \quad (2)$$

PP and RMS received SPL and SEL were measured for each logged seismic pulse after the pressure time series was band pass filtered using a 4th order elliptic filter over the frequency range 10–1000 Hz to minimize energy from other sources. The filter had a wider frequency band than needed for airgun pulses to avoid edge effects associated with narrower band elliptic filters. The RMS SPL time window, T, was determined as the interval over which the cumulative pulse energy curve rises from 5% to 95% of the total energy (Madsen, 2005). As the seismic pulse propagates through a dispersive waveguide, the time window will increase with increasing range. HARP recording were converted to absolute SPLs based on laboratory calibration of HARP hydrophones.

Transmission loss (TL) quantitatively describes the decrease in SPL of sound as it travels a distance in the ocean between source and receiver, and relates the sound's received level (RL) to its source level (SL) by the sonar equation (Urick, 1983):

$$\mathrm{RL} = \mathrm{SL} - \mathrm{TL} \quad (3)$$

Transmission loss is the sum of loss from spreading and attenuation. Spreading is a reduction of the sound levels with increased range as it geometrically spreads outward from the source distributing its energy across the region. Attenuation includes losses from absorption, scattering and leakage out of sound channels. At low frequencies (i.e., < ~100 Hz), airgun sound absorption was negligible, and the recordings were during ice-free periods during low sea state, so scattering from the air-sea interface of both waveguides was low. However, leakage and scattering caused by the frequent interaction of the sound waves at the seafloor in the shallow-water waveguide may be significant as these waves propagate long distances.

Once NMDM ranges were estimated for the pulses (see Section 2.2 below), received levels and their respective ranges were used to estimate transmission loss by fitting received levels in decibels versus the logarithm base-10 of the ranges to a line via a linear regression model. The regression coefficient, or slope (m) of the line, provides a metric of TL and is often used to describe simple spreading loss in the range-dependent equation:

$$\mathrm{TL\ (dB)} = m * \log_{10}(\mathrm{range}) \quad (4)$$

for example, cylindrical spreading (m = 10) and spherical spreading (m = 20). The regression error term, or y-intercept of the line, is the estimated source level in Eq. (3) when the slope is constant over all ranges down to 1 m.

2.2. Range estimation – normal mode dispersion modeling

The normal mode algorithm, *Kraken*, implemented in the Acoustics Toolbox (http://oalib.hlsresearch.com/), was used to generate NMDMs for the deep-water (Beaufort Sea) and shallow-water (Chukchi Sea) regions. Models for the two regions differed greatly because of the two different sound speed environments. Using the mode-specific group velocities from the models, synthetic spectrograms at various ranges were created for both deep- and shallow-water regions assuming a broadband, short duration impulsive source. A MATLAB-based tool was developed and utilized to overlay synthetic spectrograms on HARP-recorded airgun pulses from both sites to estimate the range that provided the best qualitative fit. The tool enabled an analyst to vary the amount of dispersion in the synthetic spectrogram by adjusting the propagation distance. A best-fit was determined by finding the range that produced a multi-mode spectrogram with the shape that most closely matched the modes and start/end times of the recorded seismic signal.

For the deep-water survey in 2007, modeled range estimates were compared to reported positions of the Canadian Coast Guard Ship *Louis S. St-Laurent* (*LSSL*) at specific times in the deep-water Beaufort Sea to verify range estimates. For the shallow-water survey in 2013, modeled range estimates were compared to the track lines of the marine mammal passive acoustic monitoring (PAM) vessel M/V *Norseman*, which was ~7.5 km ahead of the airgun survey vessel R/V *Geo Arctic*.

2.3. Seismic surveys and environmental model parameters

2.3.1. Deep-water Beaufort Sea

An airgun source measurement experiment was conducted in August 2009 using the seismic airgun array on the *LSSL* and a calibrated hydrophone receiver lowered to ~150 m depth from the United States Coast Guard Cutter *Healy* (Roth and Schmidt, 2010). The array, similar to the one used aboard the *LSSL* during the deep-water survey in 2007, was composed of three Sercel G-gun airguns and had a total volume of 1150 in.^{3} with a measured zero-to-peak source level of 235 dB_p re 1 μPa @ 1 m (5.75 bar-m) and peak-to-peak source level of 241 dB_{pp} re 1 μPa @ 1 m (11.75 bar-m) (Jackson, 2007; Roth and Schmidt, 2010). These recordings revealed the main pulse to be about 0.02 s in duration with most of the energy below 1000 Hz (Fig. 2). Inspection of the pulse

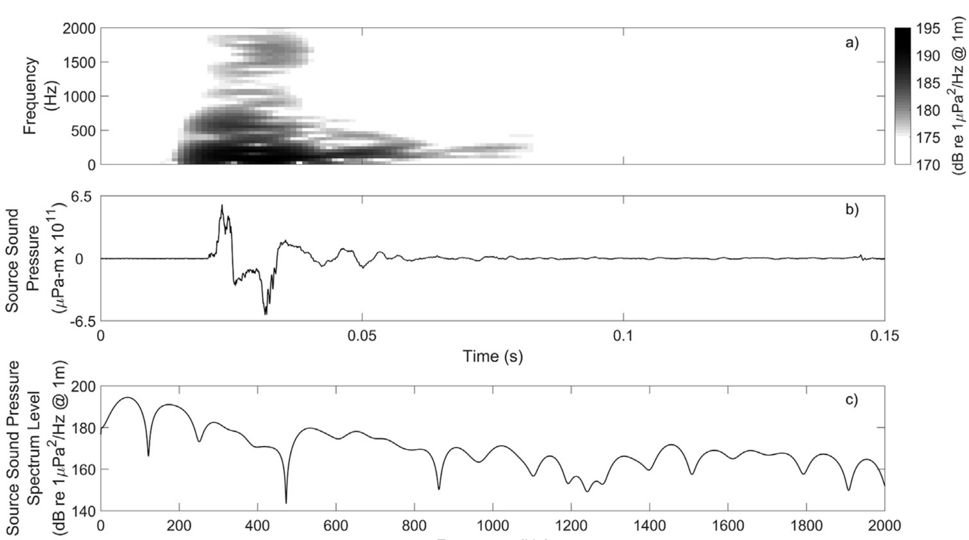

Fig. 2. Source (a) spectrogram, (b) sound pressure level time series and (c) sound pressure level frequency spectrum of a pulse from the *LSSL* airgun array corrected for spherical spreading and the calibrated hydrophone frequency response, recorded approximately 300m from the seismic source in the deep-water Beaufort Sea (from Roth and Schmidt, 2010).

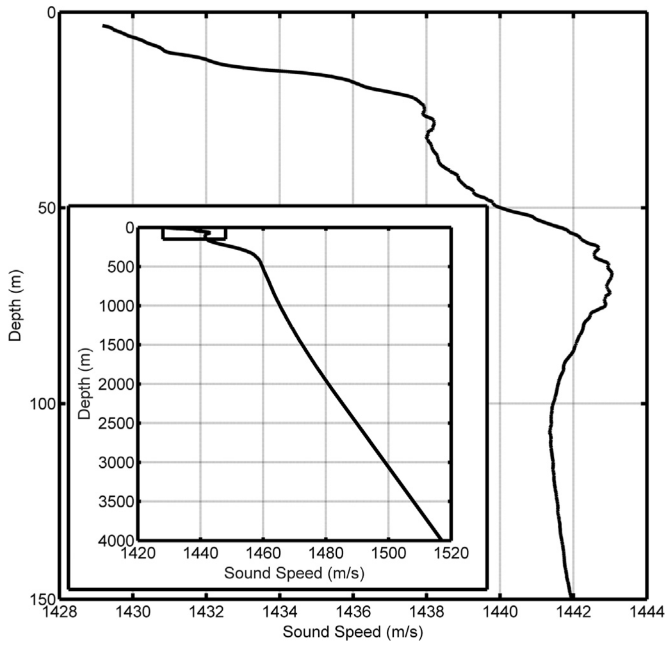

Fig. 3. Sound speed profile used to model the dispersion and range estimation for airgun pulses in the deep-water waveguide. The profile was estimated from averaged conductivity-temperature-depth (CTD) casts collected in the deep-water Beaufort Sea during the *LSSL* seismic cruise in 2007. The CTDs showed a highly variable layer in the top 150 m; below this layer, sound speed increases linearly with depth due to increasing pressure.

shows an initial increase in pressure, followed by a decrease of pressure from a reflection off the hull of the ship, and then a negative pressure air-sea interface reflection, followed by the bubble pulse.

Between 16 September and 7 October 2007, seismic pulses were produced by the *LSSL* conducting a geophysical survey in the deep-water Beaufort Sea (Fig. 1). Sound velocity casts were made during the *LSSL's* 2007 expedition from 900 to 3000 m over the survey area using an Applied Microsystems SV Plus V2 sound velocity meter with a 5000-m depth limit (Jackson, 2007). Multiple sound velocity casts below ~150 m had variability of less than ± 1 m/s and were averaged to create a sound speed profile (Fig. 3) that formed the basis for the deep-water model. The model includes a layer in which the top 50 m had higher variability around ± 5 m/s, but not enough to affect NMDM range estimation. Below this layer, the sound speed profile increases linearly with depth due to increasing pressure.

The average sound speed profile and a single layer bottom were used as inputs for sound propagation modeling. A simple bottom type with a compressional wave speed of 1800 m/s and a density of 1.6 g/cm^3 was used for the deep-water regions since basin depths greater than 3500 m and a steep continental slope suggest limited bottom interaction by the refracted seismic pulses during long-range propagation. Modeled spectrograms were qualitatively fit to acoustic data between approximately 300 and 800 km range in 10 km increments. The position of the *LSSL* was logged every half hour in the seismic watch log, allowing approximate positions within 15 min of each seismic pulse to be compared to NMDM ranges. Although the *LSSL* operated in both ice-covered and open-water conditions in the Beaufort Sea (Jackson, 2007), the path between the *LSSL* and the HARP was largely ice-free (Spreen et al., 2008; Jackson, 2007), so an air-sea interface was used as the surface of the model.

2.3.2. Shallow-water Chukchi Sea

A seismic airgun survey was conducted in support of oil and gas lease sales in the Chukchi Sea from 14 August to 31 October 2013 by TGS-NOPEC Geophysical Company. During the survey, the source vessel R/V *Geo Arctic* towed a 40-gun airgun array (26 active, 14 spare) with a discharge volume of 3280 in^3 deployed at 6 m depth and transited over a two-dimensional grid pattern (Cate et al., 2014). Seismic pulses were emitted at intervals of 8–12 s while the R/V *Geo Arctic* traveled at an average speed of 4.6 knots (8.5 km h^{-1}). Independent of the HARP recordings, acoustic recordings from an array of JASCO Applied Sciences recorders during this seismic survey show the source sound pressure levels were approximately 245 dB$_{rms}$ re 1 μPa @ 1 m (Cate et al., 2014).

The Chukchi Sea sound propagation model was constructed from a homogenous water column sound speed profile of 1465 m/s and a sediment layer with a compressional wave speed of 1900 m/s and density of 1.9 g/cm^3; where geoacoustic parameters were taken as median values for sediment based on the general local geology because no direct measurements were available (Ireland et al., 2007). The majority of the survey line was conducted on a region of the shelf with a water depth of ~70 m, and the HARP hydrophone receiver depth was 55 m. The modeled normal mode spectrograms were fit to HARP data between 35 and 100 km in 5 km increments. A smaller range increment than for the deep-water was used to accommodate the shorter survey distance on the Chukchi Shelf. Modeled range estimates were compared to reported track line positions to verify locations to within 7.5 km.

3. Results

3.1. Deep-water sound propagation in the Beaufort Sea

Airgun pulses from the *LSSL* survey in the deep-water Beaufort Sea were recorded between approximately 300 km and 750 km away and showed dispersed signal arrivals with durations extending over 4 s for the nearest pulses to almost 9 s for the farthest pulses. A spectrogram of the recorded pulses clearly shows separate modes sweeping up in frequency throughout the pulse arrivals (Fig. 4), and sound pressure amplitude time series have low signal-to-noise ratio for these arrivals because of the relatively high background sound pressure levels across this band for this region (e.g., Roth et al., 2012).

Normal-mode modeled synthetic spectrograms for the seismic source in the deep-water Beaufort Sea were calculated for 18 logged airgun bouts recorded from 16 September through 7 October 2007. An example of a synthetic spectrogram for an impulsive source 510 km away overlaid on a seismic pulse received at Site C shows a good fit to the first four modes (Fig. 5). Using NMDM for all logged bouts, range estimates were within 50 km of the positions from the *LSSL* seismic watch log.

Airgun pulse received sound pressure levels decreased with increasing range in the deep-water, near-surface waveguide of the Beaufort Sea (Fig. 6). Linear regression modeling of the received SPLs and range (Table 1) show that the propagation losses for PP and RMS SPLs are similar to spherical spreading (i.e., 20 *$\log_{10}$[range]); whereas, those for SELs are similar to cylindrical spreading (i.e., 10 *$\log_{10}$[range]). Estimated PP SPL from the y-intercept of the fitted line is about 9 dB lower than Roth and Schmidt (2010) measured, but RL variability at some ranges is up to 5 dB and the coefficient of determination, R^2, is not high, suggesting the simple regression model does not account for all the variance.

3.2. Shallow-water sound propagation in the Chukchi Sea

Seismic airgun pulses propagated in the shallow-water Chukchi Sea show modes that sweep down in frequency over time (Fig. 7), which is distinctly different from the deep-water Beaufort Sea where the modes sweep up in frequency over time. When background sound levels are low, an inflection in the first mode can be observed near 10 Hz where the modal energy above this frequency is primarily in the water column and the energy below this frequency is primarily within the seafloor.

Distances from the seismic source to the HARP obtained using

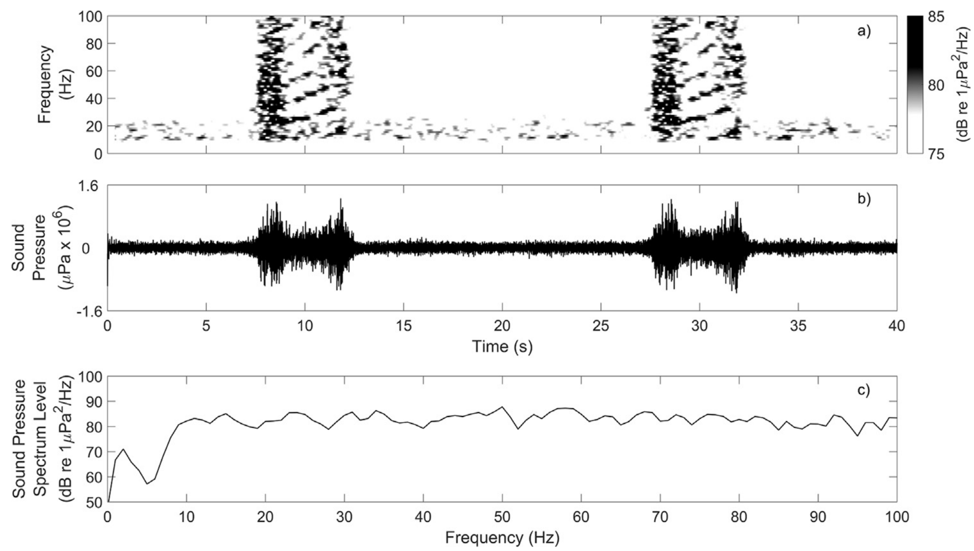

Fig. 4. Two seismic pulses recorded at Site C from the *LSSL* seismic airgun source in the deep-water Beaufort Sea approximately 507 km from the HARP: (a) spectrogram, (b) received sound pressure level time series and (c) received sound pressure spectrum level of the first pulse.

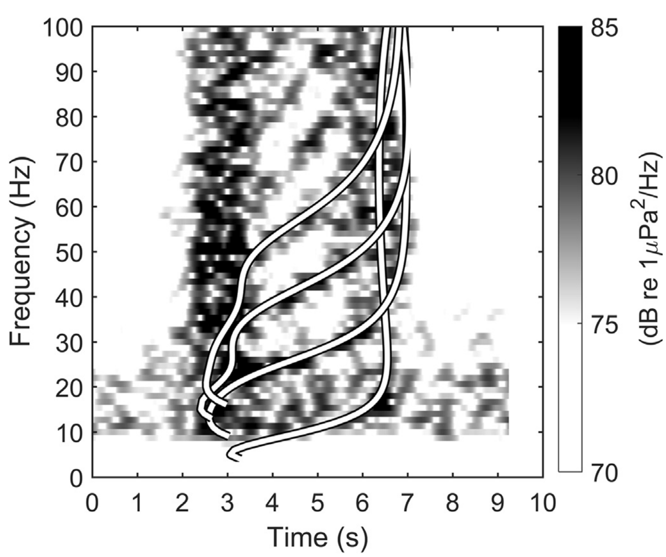

Fig. 5. Spectrogram of a seismic airgun pulse from the Beaufort Basin recorded at Site C overlaid with a synthetic spectrogram (white modes) using the NMDM and a best-fit range estimate. The best-fit model estimated the source array to be approximately 510 km from Site C; whereas, the actual distance was 507 km, which is within the 10 km resolution of the NMDM.

synthetic spectrograms from the NMDM overlaid on airgun pulses from the seismic survey ranged from approximately 35 km to 100 km for the 8 logged bouts between 23 September, 22:30:00 GMT, and 24 September 2013, 08:30:00 GMT. Pulse durations in the shallow-water waveguide increased from about 1.0 s to ~1.7 s up to 90 km range, after which pulse spreading increased more rapidly to almost 3.0 s near 100 km. A synthetic spectrogram for an impulsive source 35 km away overlaid on a seismic pulse received at Site D shows a good fit to the first two modes and perhaps the faint third mode (Fig. 8).

Airgun pulse received sound pressure levels decreased with increasing range in the shallow-water waveguide of the Chukchi Sea (Fig. 9). Linear regression modeling of the received SPLs and range (Table 2) show that the propagation losses are much greater than spherical spreading with TL regression coefficients around 50, suggesting attenuation over the shallow-water shelf is more significant than for the deep-water waveguide. Also, the exceedingly high TL regression coefficients (i.e., slope) result in TL regression errors (i.e., y-intercept) that are unrealistically too high to represent estimated source levels with more than 360 dB_{pp} re 1 μPa @ 1 m, while the coefficient of determination values, R^2, were high (~0.9) based on low variability and a good fit of the data to the modeled line.

An independent sound propagation and source verification test performed by JASCO Applied Sciences in the Chukchi Sea (Cate et al., 2014) yielded a best-fit curve of:

$$\text{RMS SPL} = -21.3 * \log_{10}(\text{range [m]}) - 0.00026*(\text{range [m]}) + 244.9\text{dB re } 1\ \mu\text{Pa @ 1m} \quad (5)$$

For ranges less than about 10 km, the propagation loss was similar to spherical spreading, but at larger distances, an additional significant range-dependent loss term (0.00026 *range [m]) was needed to fit the data. RMS SPL received levels from Site D versus the range were plotted for both NMDM estimated ranges and PAM vessel derived ranges along with JASCO's propagation curve (Fig. 10).

4. Discussion

Signal dispersion is key to understanding sound propagation in the Arctic because of the presence of acoustic waveguides for both deep-water and on-shelf propagation. In deep-water, low-frequency waves travel faster than high-frequency waves for each normal mode (Kutschale, 1977; Yang, 1984) such that an airgun impulse appears as an upswept signal when propagation ranges are > ~50 km. In contrast, low-frequency waves travel slower on the shelf than high-frequency waves for each mode (e.g., Wiggins et al., 2004) such that an airgun impulse appears as a downswept signal. In both cases, pulse spreading increased with increasing range, but was much less in the shallow-water waveguide than the deep-water waveguide due to the longer propagation ranges in the deep-water. In either case, spectrograms from single sensor (i.e., non-array) recordings can be modeled to estimate source-receiver range using the sound propagation environment and requiring only knowledge of the source frequency-temporal characteristics without needing knowledge of the source location.

Pulse spreading owing to dispersion suggests that PP and RMS SPL signal measures may be inadequate to capture the total airgun pulse energy. Pulse spreading in the deep-water waveguide presented here results in PP and RMS SPLs with an apparent ~20 *$\log_{10}$(range) transmission loss similar to spherical spreading and estimated source level difference between PP and RMS of ~9 dB as expected for quasi-continuous sinusoidal signals. In contrast, using the SEL over the

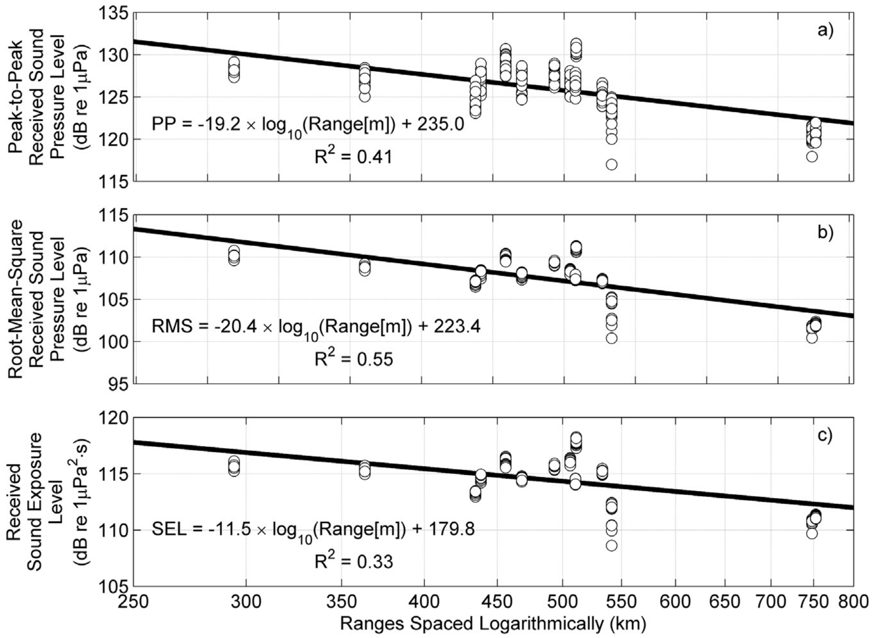

Fig. 6. Deep-water seismic airgun pulse received levels recorded at Site C versus logarithm (base-10) of the range derived from normal mode modeling. (a) PP SPL (dB_{pp} re 1 μPa); (b) RMS SPL (dB_{rms} re 1 μPa); (c) SEL (dB re 1 $\mu Pa^2 s$). The TL regression coefficients for PP and RMS SPLs are similar to spherical spreading (20), but SEL is closer to cylindrical spreading (10), retaining pulse energy as it expands in time.

Table 1
Linear regression values for plots in Fig. 6 for the transmission loss of airgun pulses in the deep-water Beaufort Sea. RL Type, TL regression coefficient (i.e., slope) and standard deviation (std), TL regression error (i.e., y-intercept) and standard deviation (std), and coefficient of determination (R^2).

RL Type	Slope (std)	y-intercept (std) dB re 1 μPa @ 1 m	R^2
PP SPL (dB_{pp} re 1 μPa)	19.2 (± 1.4)	235.0 (± 8.0)	0.41
RMS SPL (dB_{rms} re 1 μPa)	20.4 (± 1.1)	223.4 (± 6.3)	0.55
SEL (dB re 1 $\mu Pa^2 s$)	11.5 (± 1.0)	179.8 (± 5.6)	0.33

complete duration of the dispersed pulse eliminates the pulse spreading effect, yielding a much lower ~10 *$\log_{10}$(range) transmission loss, which is consistent with cylindrical spreading in an idealized two-dimensional waveguide. Given that the durations of the deep-water pulses are a function of range and were stretched to around 5 s over 500 km range, their ratio can be can be rewritten as $T \approx \text{range} * 10^{-5}\ \text{s m}^{-1}$. Inserting this relationship into Eq. (2) shows the SEL transmission loss regression coefficient and estimated source level in Table 1 are similar to what is expected from the RMS SPL measurements.

Estimates of airgun array source levels for the *LSSL* survey in the Beaufort Sea from the constant, y-axis intercept, range-independent terms of the three linear regressions resulted in estimated source SPLs lower than previously reported likely because of relatively low coefficient of determination values, $R^2 < 0.6$, indicating high variability in linearly fitting the data to the model line. The extrapolation of the linear fit to the source level at 1 m is about 6 dB less than the source PP SPL estimate of 241 dB_{pp} re 1 μPa @ 1 m measured at 300 m from the vessel (Roth and Schmidt, 2010), and may be less certain for RMS SPL and SEL.

While the coefficient of determination values, R^2, were high (~0.9) for the shallow-water Chukchi Sea, indicating a good linear fit over the ranges sampled, the transmission loss coefficient of regression and

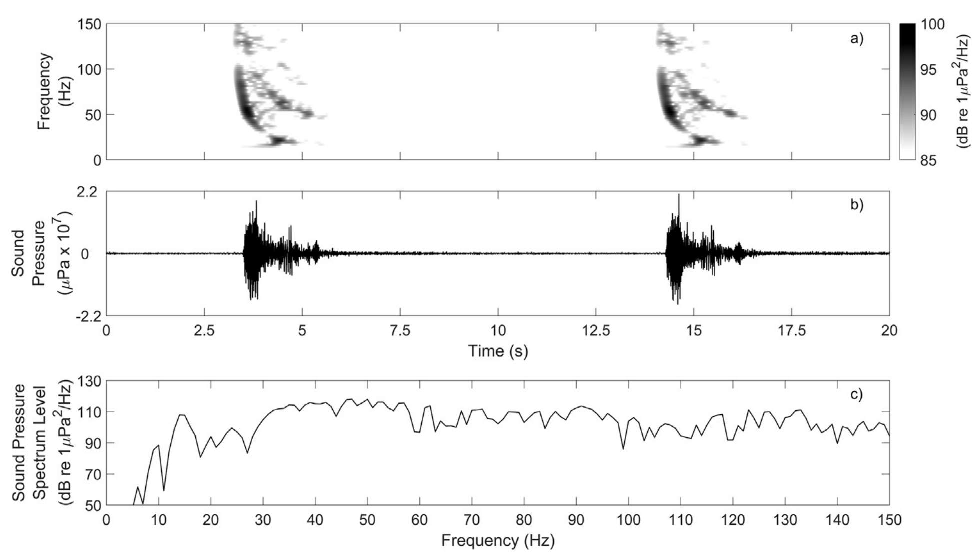

Fig. 7. Two seismic airgun pulses generated from the R/V *Geo Arctic* seismic airgun source in the shallow-water Chukchi Sea and recorded at Site D approximately 40 km from the source: (a) spectrogram, (b) received sound pressure level time series and (c) received sound pressure spectrum levels of the first pulse.

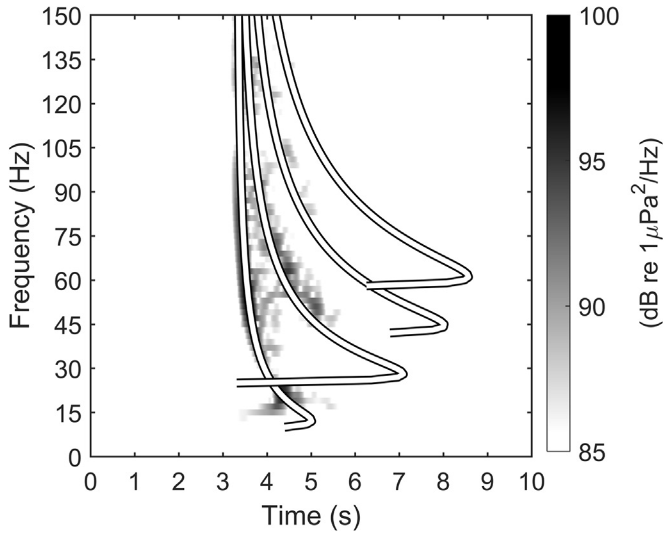

Fig. 8. Spectrogram of a seismic airgun pulse on the Chukchi Shelf recorded at Site D overlaid with a synthetic spectrogram (white modes) using the NMDM and a best-fit range estimate. The best-fit model estimated the source array to be approximately 35 km from Site D.

regression error were unrealistically too high to explain the transmission loss over the whole propagation path back to the source, suggesting energy leakage from the waveguide from an additional attenuation loss mechanism not observed in the deep-water waveguide. An independent but nearly concurrent study showed transmission loss similar to spherical spreading near the airgun source up to about 10 km, but at greater ranges up to ~80 km, significant additional attenuation losses were observed and an additional range-dependent term (i.e., ~26 dB/100 km) was needed to describe the sound pressure level loss as the airgun pulses propagated over the shelf.

The additional transmission loss could be caused by gas-saturated sediments or an elastic seafloor with shear wave speeds less than the speed of sound in the water column. In the latter case, some of the acoustic compressional wave energy is converted to shear wave energy at the water-seafloor interface which is then radiated in the seafloor and unable to re-emerge in the water column, thus reducing the energy

Table 2
Linear regression values for plots in Fig. 9 for the transmission loss of airgun pulses in the shallow-water Chukchi Sea. RL Type, TL regression coefficient (i.e., slope) and standard deviation (std), TL regression error (i.e., y-intercept) and standard deviation (std), and coefficient of determination (R^2).

RL Type	Slope (std)	y-intercept (std) dB re 1 μPa @ 1 m	R^2
PP SPL (dB_{pp} re 1 μPa)	45.9 (± 0.8)	363.6 (± 4.0)	0.86
RMS SPL (dB_{rms} re 1 μPa)	51.8 (± 0.9)	374.3 (± 4.2)	0.88
SEL (dB re 1 $\mu Pa^2 s$)	47.9 (± 0.7)	356.9 (± 3.5)	0.90

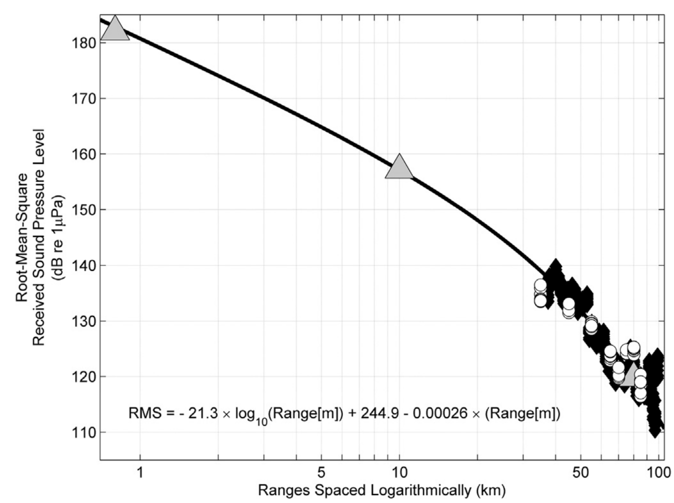

Fig. 10. Received RMS SPL from seismic airgun pulses on the Chukchi Shelf measured at Site D from Fig. 9b using ranges derived from normal mode modeling (circles) and from the M/V *Norseman* track lines (diamonds). An independent study best-fit propagation loss model with an attenuation term (26 dB/100 km) is shown as a black curve and gray triangles (Cate et al., 2014). Ranges are spaced logarithmically (base-10).

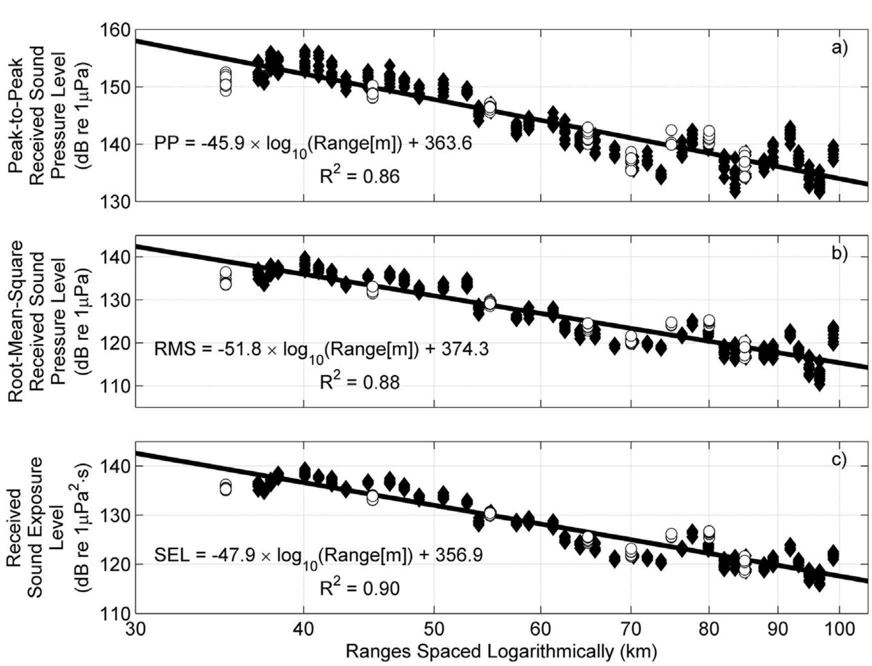

Fig. 9. Shallow-water airgun pulse received levels recorded at Site D versus the logarithm (base-10) of the range derived from normal mode modeling (circles) and from the M/V *Norseman* track lines (diamonds). (a) PP SPL (dB_{pp} re 1 μPa); (b) RMS SPL (dB_{rms} re 1 μPa); (c) SEL (dB re 1 $\mu Pa^2 s$). The TL regression coefficient (~50) is much greater than spherical spreading (20), suggesting attenuation is significant on the Chukchi Shelf.

received at the hydrophone (e.g., Ellis and Chapman, 1985). In a similar spatial-scale study on the shelf in the Bering Sea (70 m depth) with similar source frequencies (~100 Hz) to this study, TL regression coefficients were estimated to be approximately 15 over 60–80 km range (Munger et al., 2011), suggesting a much different sub-seafloor geology and less leaky waveguide in the Bering Sea than the Chukchi Sea.

In addition to environmental factors affecting transmission loss in the shallow Chukchi Sea, geometric aspects of the source could also contribute to the observed high transmission loss. For example, the shallow source depth of 6 m creates a dipole effect which generally reduces horizontal propagation compared to vertical propagation. Also, airgun arrays typically have a horizontal directivity pattern with peak sound pressure broadside to the long axis of the array, but the recordings presented here were along this axis and therefore likely resulted in reduced levels. Furthermore, depending on the configuration and aspect of the airgun array source elements, higher levels of transmission loss than from a single airgun can occur (Richardson et al., 1995).

The presence or absence of ice has a profound impact on sound transmission loss. Measurements of transmission loss conducted during the winter (Marsh and Mellen, 1963; Buck and Greene, 1964; DiNapoli and Mellen, 1986) suggest significant excess attenuation of about ~0.1 dB/km @ 100 Hz above what would be expected from an ice-free deep sound channel (Urick, 1983). Scattering from the rough under surface of the ice cover is the dominant cause of excess attenuation. During open-water conditions, Arctic sound propagation becomes comparable to the deep sound channel (Thode et al., 2010).

Diminished ice in the Arctic Ocean allows for longer range sound propagation, and during these ice-free periods, seismic surveys often occur and overlap with the annual westward migration of the bowhead whale (*Balaena mysticetus*) and fall subsistence hunt of native communities along the Beaufort and Chukchi Seas. In the presence of seismic airgun activity, bowhead whales have exhibited signs of behavioral disturbance and avoidance of the survey area with received SPLs ranging from ~120 to ~170 dB_{rms} re 1 μPa (Richardson et al., 1986, 1999; Ljungblad et al., 1988; McCauley et al., 2000; Miller et al., 2005), with context (migrating vs. feeding) playing a significant role in the severity of the response. For example, migrating bowhead whales have been shown to move away from seismic airguns at low received levels (~120 dB_{rms} re 1 μPa) (Miller et al., 1999; Richardson et al., 1999). From our study, using a source SPL of 245 dB_{rms} re 1 μPa @ 1 m (i.e., from the R/V *Geo Arctic*'s 26-active-gun airgun array), we estimate a received SPL of 120 dB_{rms} re 1 μPa at ~135 km range in the Beaufort Basin and ~80 km in the Chukchi Sea, suggesting a disturbance area for bowhead whales in the deep-water basin (57,256 km^2) that is more than twice as large as over the shallow-water shelf (20,106 km^2 > the size of the state of New Jersey), potentially causing displacement from important migratory routes, feeding areas and traditional hunting grounds. Furthermore, because bowhead whale calls overlap the low-frequency band of seismic airgun pulses (Clark and Johnson, 1984), auditory masking of the calls from the seismic pulses may interfere with the important functions of those calls.

5. Conclusions

Seismic airgun pulses propagate long distances underwater owing to their low frequency (i.e., low absorption) and high sound pressure levels. In the open-water Arctic, environmental factors create acoustic waveguides which affect how signals propagate. Ideal waveguides suggest low transmission losses similar to cylindrical spreading, but also predict waveform dispersion spreading the signal's energy over long periods. Increasing signal duration in a deep-water waveguide effectively increases transmission losses for PP and RMS SPLs to those similar to spherical spreading. On the other hand, SEL measurements account for signal duration and show propagation losses similar to cylindrical spreading, suggesting SEL may be a better metric to describe how impulses such as airguns propagate in dispersive environments.

Two different types of Arctic waveguides provided two different types of dispersed airgun pulses. The deep-water Beaufort Sea near-surface waveguide produces upsweeping signals with many modes over 100's of km; whereas, the shallow-water Chukchi Sea produces down-sweeping signals that attenuate at a greater rate over a shorter distance (10's of km). The additional loss term needed for the shallow-water waveguide is likely due to the signal's acoustic energy being lost in a seafloor with low shear speed, and therefore low shear strength, but geometric aspects of the airgun array also may have contributed to the observed high transmission loss.

Measuring and modeling sound propagation provides a better understanding of how seismic activities influence ambient noise levels, and potentially wildlife, across large spatial scales. Received sound pressure levels are often measured or calculated to determine the size of an exclusion or safety zone radius, a mitigation measure employed to protect marine mammals from injurious or disturbing sound levels. As a result, understanding sound propagation in the Arctic can provide resource managers with the necessary tools and information to develop effective mitigation measures for anthropogenic noise pollution.

Acknowledgements

We thank Ethan Roth, Chris Garsha and Josh Jones of the Marine Physical Laboratory at Scripps Institution of Oceanography for their technical support with HARP operations. We thank the Bob Small of the Alaska Department of Fish and Game, the Coastal Impact Assistance Program of the U.S. Fish and Wildlife Service, and Craig George and Robert Suydam of the North Slope Borough Department of Wildlife Management for providing the funding to make this study possible. We thank Larry Mayer of the University of New Hampshire, John Kemp of Woods Hole Oceanographic Institution and the crew of the U.S. Coast Guard Cutter *Healy* for HARP field and logistical support during 2007–2008 and 2012–2013, as well as Robert S. Pickart of Woods Hole Oceanographic Institution for the 2012–2013 season. We also thank John Shimeld of the Geological Survey of Canada for the field report and seismic watch log for the 2007 *LSSL* seismic cruise. We thank Jon Biggar of the Canadian Hydrographic Service for the sound velocity profiles for the 2007 *LSSL* seismic cruise and David Mosher of the Geological Survey of Canada for airgun source calibration information. We thank Ethan Roth and Val Schmidt for the collection of the seismic source signature data and the U.S. Coast Guard for their support for field programs. We thank six anonymous peer-reviewers whose helpful comments improved the clarity of this manuscript.

References

Bongiovanni, K.P., Badley, M., Siegmann, W.L., 1995. Shallow-water sediment layer structure and composition effects on range-dependent acoustic propagation at the Atlantic-Generating Station (AGS) site. J. Acoust. Soc. Am. 98, 2249–2261.

Buck, B.M., Greene, C.R., 1964. Arctic deep-water propagation Measurements. J. Acoust. Soc. Am. 36, 1526–1533.

Cate, J.R., Smultea, M., Blees, M., Larson, M., Simpson, S., Jefferson, T., Steckler, D., 2014. 90-Day Report of Marine Mammal Monitoring and Mitigation during a 2D Seismic Survey by TGS in the Chukchi Sea, August through October 2013. AES Doc. No. 15416-04 13-185. Prepared by ASRC Energy Services, Smultea Environmental Sciences, Clymene Enterprises and Entiat River Technologies for TGS-NOPEC Geophysical Company, National Marine Fisheries Service and U.S. Fish and Wildlife Service. 122 p. + Appendices. 〈http://www.nmfs.noaa.gov/pr/pdfs/permits/tgs_90dayreport.pdf〉 (Last viewed 2/14/2018).

Clark, C.W., Johnson, J.H., 1984. The sounds of the bowhead whale, *Balaena mysticetus*, during the spring migrations of 1979 and 1980 (1984). Can. J. Zool. 62 (7), 1436–1441. https://doi.org/10.1139/z84-206.

DiNapoli, F.R., Mellen, R.H., 1986. Low Frequency Attenuation in the Arctic Ocean. In: Akal, T., Berkson, J. (Eds.), Ocean Seismo-Acoustics. Springer, US, pp. 387–395.

Dragoset, W., 1984. A comprehensive method for evaluating the design of air guns and air gun arrays. Geophys.: Lead. Edge 3, 52–61.

Dragoset, W., 2000. Introduction to air guns and air-gun arrays. Geophys.: Lead. Edge 19, 892–897.

Ellis, D.D., Chapman, D.M.F., 1985. A simple shallow water propagation model including

shear wave effects. J. Acoust. Soc. Am. 78 (6), 2087–2095.
Gavrilov, A.N., Mikhalevsky, P.N., 2006. Low-frequency acoustic propagation loss in the Arctic Ocean: results of the Arctic climate observations using underwater sound experiment. J. Acoust. Soc. Am. 119, 3694–3706.
Hildebrand, J.A., 2009. Anthropogenic and natural sources of ambient noise in the ocean. Mar. Ecol. Prog. Ser. 395, 5–20.
Ireland, D., Hannay, D., Rodrigues R., Patterson, H., Haley, B., Hunter, A., Jankowski, M., Funk, D.W., 2007. Marine mammal monitoring and mitigation during open water seismic exploration by GX Technology in the Chukchi Sea, October—November 2006: 90-day report, LGL Draft Rep. P891-1. Rep. from LGL Alaska Research Associates Inc., Anchorage, AK, LGL Ltd., King City, Ont., and JASCO Research, Ltd., Victoria, B.S., Can. for GX Technology, Houston, TX, and Nat. Mar. Fish. Serv., Silver Spring, MD. 118 pp. ⟨http://www.nmfs.noaa.gov/pr/pdfs/permits/gxt_90day_report.pdf⟩ (Last viewed 5/31/2018).
Jackson, R.H., 2007. Field Report for 2007 the CCGS Louis S. St-Laurent seismic cruise to the Canada Basin. Geological Survey of Canada, Open File 5818. pp. 143.
Jensen, F.B., Kuperman, W.A., Porter, M.B., Schmidt, H., 2000. Computational ocean acoustic. Springer Science & Business Media, pp. 466.
Kutschale, H.W., 1977. Low-Frequency Propagation in the Ice-Covered Arctic Ocean. In: International Workshop on Low-Frequency Propagation and Noise, Woods Hole, Massachusetts, 14-19 October 1974 (Vol. 2, p. 683). Department of the Navy.
LePage, K., Schmidt, H., 1994. Modeling of low-frequency transmission loss in the central Arctic. J. Acoust. Soc. Am. 96, 1783–1795.
Ljungblad, D.K., Würsig, B., Swartz, S.L., Keene, J.M., 1988. Observations on the behavioral responses of bowhead whales (*Balaena mysticetus*) to active geophysical vessels in the Alaskan Beaufort Sea. Arctic 41, 183–184.
Madsen, P.T., 2005. Marine mammals and noise: problems with root mean square sound pressure levels for transients. J. Acoust. Soc. Am. 117 (6), 3952–3957.
Marsh, H.W., Mellen, R.H., 1963. Underwater sound propagation in the Arctic Ocean. J. Acoust. Soc. Am. 35, 552–563.
McCauley, R.D., Fewtrell, J., Duncan, A.J., Jenner, C., Jenner, M.-N., Penrose, J.D., et al., 2000. Marine seismic surveys: a study of environmental implications. Aust. Pet. Prod. Explor. Assoc. J. 40, 692–708.
Medwin, H., Clay, C.S., 1998. Fundamentals of acoustical oceanography. Academic Press, Boston, pp. 468 (p.).
Miller, G.W., Elliott, R.E., Koski, W.R., Moulton, V.D., Richardson, W.J., 1999. ("Whales," p. 51 to 5-109) In: Richardson, W.J. (Ed.), Marine mammal and acoustical monitoring of Western Geophysical's open-water seismic program in the Alaskan Beaufort Sea, 1998. LGL Rep. TA2230-3. Rep. from LGL Ltd., King City, Ont., and Greeneridge Sciences Inc., Santa Barbara, CA, for Western Geophysical, Houston, TX, and U.S. Nat. Mar. Fish. Serv. Anchorage, AK, and Silver Spring, MD, pp. 390 ("Whales," p. 51 to 5-109).
Miller, G.W., Moulton, V.D., Davis, R.A., Holst, M., Millman, P., MacGillivray, A., Hannay, D., 2005. Monitoring seismic effects on marine mammals—southeastern Beaufort Sea, 2001–2002. In: Armsworthy, S.L., Cranford, P.J., Lee, K. (Eds.), Offshore oil and gas development effects monitoring/approaches and technologies. Battelle Press, Columbus, Ohio, pp. 511–542 (pp).
Munger, L.M., Wiggins, S.M., Hildebrand, J.A., 2011. North Pacific right whale up-call source levels and propagation distance on the southeastern Bering Sea shelf. J. Acoust. Soc. Am. 129, 4046–4054.
Nieukirk, S.L., Stafford, K.M., Mellinger, D.K., Dziak, R.P., Fox, C.G., 2004. Low-frequency whale and seismic airgun sounds recorded in the mid-Atlantic Ocean. J. Acoust. Soc. Am. 115, 1832–1843.
Richardson, W.J., Würsig, B., Greene Jr., C.R., 1986. Reactions of bowhead whales, *Balaena mysticetus*, to seismic exploration in the Canadian Beaufort Sea. J. Acoust. Soc. Am. 79, 1117–1128.
Richardson, W.J., Greene Jr., C.R., Malme, C.I., Thomson, D.H., 1995. Marine mammals and noise. Academic Press, San Diego, pp. 576 (p).
Richardson, W.J., Miller, G.W., Greene Jr., C.R., 1999. Displacement of migrating bowhead whales by sounds from seismic surveys in shallow waters of the Beaufort Sea. J. Acoust. Soc. Am. 106, 2281.
Roth, E.H., Hildebrand, J.A., Wiggins, S.M., Ross, D., 2012. "Underwater ambient noise on the Chukchi Sea continental slope from. J. Acoust. Soc. Am. 131, 2006–2009 (104-110).
Roth, E.H., Schmidt, V., 2010. U.S. Geological Survey, Coastal and Marine Geology, Report on Cooperative Agreement G09AC00352: Noise levels generated by research icebreakers and marine seismic sources in the deep-water, Arctic Ocean, Marine Physical Laboratory Technical Memorandum 527, Scripps Institution of Oceanography, La Jolla, CA.
Southall, B.L., Bowles, A.E., Ellison, W.T., Finneran, J.J., Gentry, R.L., Greene Jr, C.R., Kastak, D., et al., 2007. Marine mammal noise exposure criteria: initial scientific recommendations. Aquat. Mamm. 33, 411–521.
Spreen, G., Kaleschke, L., Heygster, G., 2008. Sea ice remote sensing using AMSR-E 89 GHz channels (C02S03). J. Geophys. Res. 113. https://doi.org/10.1029/1005JC003384.
Thode, A., Kim, K.H., Greene Jr., C.R., Roth, E.H., 2010. Long range transmission loss of broadband seismic pulses in the Arctic under ice-free conditions. J. Acoust. Soc. Am. 128, 181–187.
Turner, S., Zykov, M., MacGillivray, A., 2006. Preliminary acoustic level measurements of airgun sources from Conoco Phillips' 2006 seismic survey in Alaskan Chukchi Sea, JASCO Research, Victoria, BC. ⟨http://www.nmfs.noaa.gov/pr/pdfs/permits/conocophillips_report.pdf⟩ (Last viewed 5/31/2018).
Urick, R.J., 1983. Principles of underwater sound. McGraw-Hill, New York, pp. 423 (p).
Welch, P.D., 1967. The use of fast Fourier transform for the estimation of power spectra: a method based on a time averaging over short, modified periodgrams. IEEE T Acoust. Speech 15, 70–73.
Wiggins, S.M., McDonald, M.A., Munger, L.M., Moore, S.E., Hildebrand, J.A., 2004. Waveguide propagation allows range estimates for North Pacific right whales in the Bering Sea. Can. Acoust. 32, 146–154.
Wiggins, S.M., Hildebrand, J.A., 2007. High-frequency acoustic recording package (HARP) for broadband, long-term marine mammal monitoring. In: International Symposium on Underwater Technology 2007. International Workshop on Scientific Use of Submarine Cables and Related Technologies 2007, pp. 551–557.
Yang, T.C., 1984. Dispersion and ranging of transient signals in the Arctic Ocean. J. Acoust. Soc. Am. 76, 262–273.